

Influence of Operating Parameters on Unbalance in Rotating Machinery Using Response Surface Method

Ameya M. Mahadeshwar^{1, *}, Sangram S. Patil¹, Vishwadeep C. Handikherkar¹, Vikas M. Phalle¹

¹ Veermata Jijabai Technological Institute, H R Mahajani Marg, Matunga, Mumbai, 400019, Maharashtra

Wide range of rotating machinery contains an inherent amount of unbalance which leads to increase in the vibration level and related faults. In this work, the effect of different operating conditions viz. the unbalanced weight, radius, speed and position of the rotor disc on the unbalance in rotating machine are studied experimentally and analyzed by using Response Surface Methodology (RSM). RSM is a technique which consists of mathematical and statistical methods to develop the relationship between the inputs and outputs of a system by distinct functions. L27 Orthogonal Array (OA) was developed by using Design of Experiments (DOE) according to which experimentation has been carried out. Three accelerometer sensors were mounted to record the vibration responses (accelerations) in radially vertical, horizontal and axial directions. The responses recorded as root mean square values are then analysed using RSM. The relationship between response and operating factors has been established by developing a second order, non-linear mathematical model. Analysis of variance (ANOVA) has been performed for verification of the developed mathematical models. Results obtained from the analysis show that the unbalance weight and speed are most significant operating conditions that contribute the most to the effect the unbalance has on the rotating spindle.

Keywords: Mechanical unbalance, response surface method, rotating machinery, ANOVA, design of experiments.

1 Introduction

The most common cause of excessive vibration is the rotor unbalance. Unbalance results from the fact that the centre of gravity of a rotating member does not coincide with the center of rotation. This causes the creation of a centrifugal force vector pointing radially outward from the center of rotation and rotating at a speed equal to the speed of the rotating member itself. Several likely sources of unbalance are, manufacturing problems, such as non-uniform castings, cocked assembly, bent shafts and non-concentric machining; non-symmetrical reduction of mass of the rotating element from wear, erosion, corrosion, or blade breakage; non-symmetrical mass addition, such as product buildup on pump or internal misalignment; application of an external force large enough to bend the shaft or rotor. The unbalance leads to a heavy spot on the rotor. The nonlinear dynamic behaviour for a plain journal bearing rotating with high speed was analysed by Belhamra et al. and they observed that the dynamic behaviour of a shaft that rotates with higher velocity is nonlinear that for poor eccentricity of unbalance¹. Response of unbalance failure modes on electric and vibration current using tribological approach has been reported by Erol et al.². The vibrations in the vicinity of resonance conditions of a rotor with 6 degrees of freedom in linear homogeneous elastoviscous field were studied by Jivkov and Zahariev³. A theoretical formulation of the effect of mechanical unbalance on the analytical expressions of radial vibration and stator current was shown by Salah et al.⁴.

The RSM works by producing a response for a input that is pre-defined. In this section, the inputs are the factors to be checked and the response is the output measured data. An estimation model of the input factors and the response, called a response surface equation, is created. Due to it, the method of optimization works on the response

surface. The RSM has benefits, as it is easy to implement while computing parallelly and also the sensitivity of factors can be checked easily. The RSM was used to design hydro-forming process and an optimization strategy was developed by Di Lorenzo et al. The optimal internal pressure curve was achieved in the hydro forming of steel tubes, with a moving least squares method by hybridizing steepest descent method⁵. In a rotor bearing system, RSM was applied for fault diagnosis by Kankar et al. The RSM was used to check the effect of design and operating factors on the vibration sign of a system⁶. Effect of localized defects on fault diagnosis of high speed rolling element bearings with the help of RSM was performed by Kankar et al. Integrated factor impacts had been checked and their effects have been accounted with DOE and RSM is utilised to estimate the dynamic response of the system⁷. Patil et al. applied RSM applied to establish the analytical model for attaining the maximum phase shift in a coriolis mass flow sensor (CMFS). Experimentation was carried out to utilize data generated to develop of mathematical model to correlate the various design factors such as sensor location; drive frequency, mass flow rate of CMFS through Response Surface Methodology⁸. Kikuchi and Takayama utilised a multi-variate spline interpolation formulated RSM to evaluate the authenticity of pharmaceutical products. They utilised a bootstrap resampling method along with a Kohonen's self-organizing map to evaluate the confidence levels of the optimal formulation⁸. Zeng et al. used the RSM to optimize the roll profile design for cold roll forming. The objective function was taken as the springback angle and constrain condition was taken as maximum edge membrane longitudinal strains for satisfying the high forming accuracy and minimum roll stands for efficiency, and performed the optimisation⁹. The RSM has been utilised for spring-back control of sheet-metal forming by Wei et al. There were two objective functions springback and thickness deformation. To minimize them collectively, a multi-objective genetic algorithm has been employed to site the optimal solution¹⁰. The response surface method was applied for optimizing a dispersive liquid liquid micro extraction (DLLME) of water soluble components by Sereshti et al. Full factorial experiments were used to determine the significant factors and their interactions¹¹. Rauf et al. used the RSM for photolytic decolorization and data optimization. How the presence of some ions affected the decolorisation of the dye was checked¹². Tang et al. applied the RSM for optimization of the tool shape. They had used a neural network to express RSM function to overcome the shortcoming of a quadratic polynomial model in solving non-linear problems¹³. An artificial neural network (ANN) based RSM for structural reliability analysis was suggested by Cheng et al. The method is used along with uniform design method by virtue of which the quality of training dataset is improved and computation becomes more efficient¹⁴. Hou et al. used the Taguchi method along with the RSM and genetic algorithm to optimise the wet-type mechanical process used to produce nano-particle¹⁵. Tir and Moulai-Mostefa studied electro-coagulation process with sacrificial aluminium anode with the aim of reducing turbidity and chemical oxygen demand (COD). Response surface method was used to find the optimal values of the turbidity and COD¹⁶. Choorit et al. utilised box-behnken design with three variables at three levels to describe the nature of response

surface in order to study demineralisation efficiency in shrimp shells¹⁷. This method has been largely used in large variety of applications like optimization of design parameters, prediction of response and validation of model. But as of now, the literature concerning to its use in analysis of effect of unbalance in rotating machine is rare. Hence, the current work is a first effort in the printed literature, to illustrate use of RSM to analyse of effect of unbalance in rotating machine. This involves analyzing the various operating factors such as position, unbalance weight, radius, speed, through RSM, using the data that is acquired by experimentation. The analysis of variance (ANOVA) test is used to check the acceptability of the developed model.

2 Response Surface Methodology (RSM)

An experimenter is about to study a system for which there is a mathematical equation relating the expected value of a response $\eta = E(y)$ to the experimental variables x_1, x_2, \dots, x_k ,

$$\eta = f(\theta_1, \theta_2, \dots, \theta_p; x_1, x_2, \dots, x_k) \quad (1)$$

where $\theta_1, \theta_2, \dots, \theta_p$ are the parameters of the system. For example, in a chemical reaction the response could be the yield; the variables might include temperature, pressure, and pH; and the parameters might include the reaction rate constant and the heat transfer coefficient. Of course, for each experimental run, more than one response may be measured; for example, cost may be measured in addition to yield¹⁸. It is likely, especially in complex situations, that the exact form of the response function f in Equation 1 will be unknown. In fact, a good case can be made for the claim that it is never known exactly. Furthermore, in many circumstances, any attempt to develop one could not be justified from an economic point of view.

For many purposes, consideration of the possible forms of the true function f is unnecessary. A flexible graduating function g (for example, a polynomial) will often be satisfactory to express the relationship between the response η and the k important variables x_1, x_2, \dots, x_k . In other words, g is an adequate approximation of f over the region of experimentation. The two most common forms of g are the first-order polynomial,

$$\eta = \beta_0 + \beta_1 x_1 + \beta_2 x_2 + \dots + \beta_k x_k \quad (2)$$

and the second order polynomial

$$\eta = \beta_0 + \beta_1 x_1 + \beta_2 x_2 + \dots + \beta_k x_k + \beta_{12} x_1 x_2 + \beta_{13} x_1 x_3 + \dots + \beta_{k-1,k} x_{k-1} x_k + \beta_{11} x_1^2 + \beta_{22} x_2^2 + \dots + \beta_{kk} x_k^2 \quad (3)$$

The coefficients $\beta_0, \beta_1, \beta_2, \dots$ are parameters to be estimated from the data. If transformations of the x 's and the y 's are considered, the flexibility of such first-order and second order models is increased substantially¹⁹. For $k=2$ experimental variables, these general polynomials reduce to,

$$\eta = \beta_0 + \beta_1 x_1 + \beta_2 x_2 \quad (4)$$

and,

$$\eta = \beta_0 + \beta_1 x_1 + \beta_2 x_2 + \beta_{12} x_1 x_2 + \beta_{11} x_1^2 + \beta_{22} x_2^2 \quad (5)$$

Response surface plots are 3D (3 dimensional) graphs that represent an operational relation between a dependent variable (Y), and two independent variables (X and Z) instead of depicting the single data points. These plots are helpful in regression analysis for analyzing the relationship between a dependent and two independent variables.

3 Design of Experiments

Experimentation has been carried out on Machinery Fault Simulator (MFS) as shown in figure 1, with the designed experiments, Design of Experiments being done on Design Expert²⁰ software.

The factors have been decided based upon the equation,

$$F = mr\omega^2 \quad (6)$$

where, m is the unbalance weight, r is the radius at which unbalance weight is placed and ω is the speed of rotation,

Along with the above factors, position of the disc on the shaft is also analysed and so 4 factors are selected. Response Surface Method is selected after performing literature survey, based on the advantages predictive accuracy, quality of optimum.

In RSM, Box-Behnken design is selected for the based on the criteria that it requires only three levels per factor whereas central composite design (CCD) requires 5 levels of each factors which is not feasible in this case. Factors at their respective levels have been decided as per literature review and available resources are shown in actual and coded units as shown in Table 1.

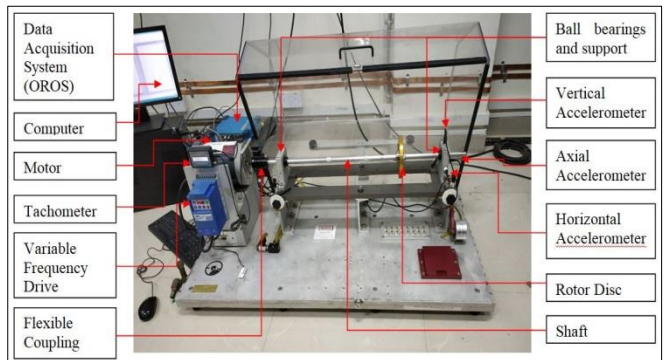


Figure 1. Experimental setup.

Table 1. Factors and their respective levels.

Factor	Factors Coded	Level 1	Level 2	Level 3
A	Position	-1	0	1
B	Unbalance Weight (gm)	1/4	1/2	3/4
C	Radius (cm)	0	10.25	20.028
D	Speed (rpm)	4.25	5.2	6.15
		900	1800	2700

Response is the acceleration values measured with the help of accelerometer sensors mounted in radially vertical, horizontal and axial directions, which are measured as signals which are converted further into root mean square (rms) values of signals using Matlab²¹ software.

Based on the factors and the levels above, L27 Orthogonal Array is developed for Response Surface Method as shown in Table 2.

4 Experimentation

The experimental setup consisted of Machinery Fault Simulator (MFS), shown in Figure 1, it consists of a motor connected to a shaft supported between two ball bearings connected with a flexible coupling. A disc is mounted on the shaft at three positions alternatively with unbalance weight at two radial positions, as per design of experiments. The disc has only two levels for variation of radii viz. 4.25 cm and 6.15 cm so the reading are taken at these levels assigned to levels 1 and 3 and are interpolated for level 2 i.e. 5.2 cm. For experimentation, three accelerometers were mounted, first radially in vertical direction, second radially in horizontal direction and third one in axial direction. Signals were acquired using Data Acquisition System (OROS) and then recorded as signal files in NVGate²² software provided with the Machinery Fault Simulator. System is aligned properly. Flexible coupling is used to connect motor to the shaft to avoid transmission of any misalignment from shaft to motor or vice versa. The signal files were analysed using Matlab²¹ and root mean square (rms) values were generated. These values as generated against the designed experiments are shown in Table 3.

Table 2. L27 orthogonal array of position, unbalance weight, radius, speed.

Sr. No.	Position	Unbalance Weight	Radius	Speed
1	0.25	0	5.2	1800
2	0.75	0	5.2	1800
3	0.25	20.028	5.2	1800
4	0.75	20.028	5.2	1800
5	0.5	10.014	4.25	900
6	0.5	10.014	6.15	900
7	0.5	10.014	4.25	2700
8	0.5	10.014	6.15	2700
9	0.25	10.014	5.2	900
10	0.75	10.014	5.2	900
11	0.25	10.014	5.2	2700
12	0.75	10.014	5.2	2700
13	0.5	0	4.25	1800
14	0.5	20.028	4.25	1800
15	0.5	0	6.15	1800
16	0.5	20.028	6.15	1800
17	0.25	10.014	4.25	1800
18	0.75	10.014	4.25	1800
19	0.25	10.014	6.15	1800
20	0.75	10.014	6.15	1800
21	0.5	0	5.2	900
22	0.5	20.028	5.2	900
23	0.5	0	5.2	2700
24	0.5	20.028	5.2	2700
25	0.5	10.014	5.2	1800
26	0.5	10.014	5.2	1800
27	0.5	10.014	5.2	1800

Table 3. L27 orthogonal array with results generated from MFS.

Sr. No.	Position	UW	Radius	Speed	rms		
					v(m/s ²)	h(m/s ²)	a(m/s ²)
1	0.25	0	5.2	1800	0.6384	0.786795	1.01185
2	0.75	0	5.2	1800	0.84218	0.928055	1.18805
3	0.25	20.028	5.2	1800	3.5029	2.15915	2.03195
4	0.75	20.028	5.2	1800	4.5535	1.964265	1.4273
5	0.5	10.014	4.25	900	0.2002	0.501	0.3021
6	0.5	10.014	6.15	900	0.2403	0.62921	0.29579
7	0.5	10.014	4.25	2700	2.44	6.0366	4.3776
8	0.5	10.014	6.15	2700	2.4506	8.5243	4.7178
9	0.25	10.014	5.2	900	0.203755	0.420095	0.347845
10	0.75	10.014	5.2	900	0.2772	0.69784	0.4314615
11	0.25	10.014	5.2	2700	2.5525	3.33355	3.867925
12	0.75	10.014	5.2	2700	1.2728	5.7013	3.041315
13	0.5	0	4.25	1800	0.39696	0.6369	0.90408
14	0.5	20.028	4.25	1800	4.1254	1.8898	1.3884
15	0.5	0	6.15	1800	0.43722	0.64335	0.59556
16	0.5	20.028	6.15	1800	5.4898	2.3386	1.462

17	0.25	10.014	4.25	1800	1.5335	1.1889	1.30912
18	0.75	10.014	4.25	1800	2.0645	1.082836	1.1201
19	0.25	10.014	6.15	1800	2.0833	1.4209	1.4719
20	0.75	10.014	6.15	1800	2.9966	1.285	1.14159
21	0.5	0	5.2	900	0.204235	0.381385	0.39925
22	0.5	20.028	5.2	900	0.288425	0.9677	0.44882
23	0.5	0	5.2	2700	0.66527	1.3746	1.5601
24	0.5	20.028	5.2	2700	9.33785	15.67385	8.0834
25	0.5	10.014	5.2	1800	2.70725	1.401495	1.2507
26	0.5	10.014	5.2	1800	2.70725	1.401495	1.2507
27	0.5	10.014	5.2	1800	2.70725	1.401495	1.2507

5 Results and Discussion

5.1 Response Surface Plots

For L27 Orthogonal Array, Response Surface Method was analyzed in Design Expert software, and surface plots were obtained. In these surface plots vertical, horizontal and axial responses (accelerations) obtained from accelerometer sensors mounted on the frame are plotted on Y axis, whereas the operating parameters are taken along X and Z axes sequentially.

Figures 2(a), 2(b) and 2(c) represent the vertical, horizontal and axial responses respectively vs. unbalance weight (factor B) and position (factor A), where radius (factor C) and speed (factor D) are held constant at 5.2 cm and 1800 rpm respectively. For vertical response, with respect to the unbalance weight, for position at 0.75, as the unbalance weight increases, the response increases from 0.4 m/s² at 0 gm to 5 m/s² at 20.028 gm, similar trend is observed at position levels 1 and 2. Whereas with respect to position, for unbalance weight at 20.028 gm, response increases from 4 m/s² at position 0.25 m/s² to 5 m/s² at position 0.5 and decreases to 4.6 m/s² at position 0.75, similar trend is observed at unbalance weight levels 1 and 2. For horizontal response, for position at 0.75, as the unbalance weight increases, the response increases from 0 m/s² at 0 gm to 2.5 m/s² at 20.028 gm,

similar trend is observed at position levels 1 and 2. Whereas with respect to position, for unbalance weight at 20.028 gm, response increases from 2.5 m/s² at position 0.25 to 3.5 m/s² at position 0.5 and decreases to 2.5 m/s² at position 0.75, similar trend is observed at unbalance weight levels 1 and 2. For axial response, for position at 0.75, as the unbalance weight increases, the response increases from 0.4 m/s² at 0 gm to 1.8 m/s² at 20.028 gm, similar trend is observed at position levels 1 and 2. Whereas with respect to position, for unbalance weight at 20.028 gm, response varies from 2.2 m/s² at position 0.25 to 1.8 m/s² at position 0.75, similar trend is observed at unbalance weight levels 1 and 2.

Figures 3(a), 3(b) and 3(c) represent the vertical, horizontal and axial responses respectively vs. speed (factor D) and position (factor A), where unbalance weight (factors B) and radius (factor C) are held constant at 10.25 gm and 5.2 cm respectively. For vertical response at position 0.5, with respect to the speed, the response increases from 0 m/s² at 900 rpm to 2.6 m/s² at 2700 rpm, similar trend is observed at position levels 1 and 2. Whereas with respect to position, for speed at 2700 rpm, response increases from 2.6 m/s² at to 3.4 m/s² at then decreases to 2.6 m/s² at, similar trend is observed at speed levels 1 and 2.

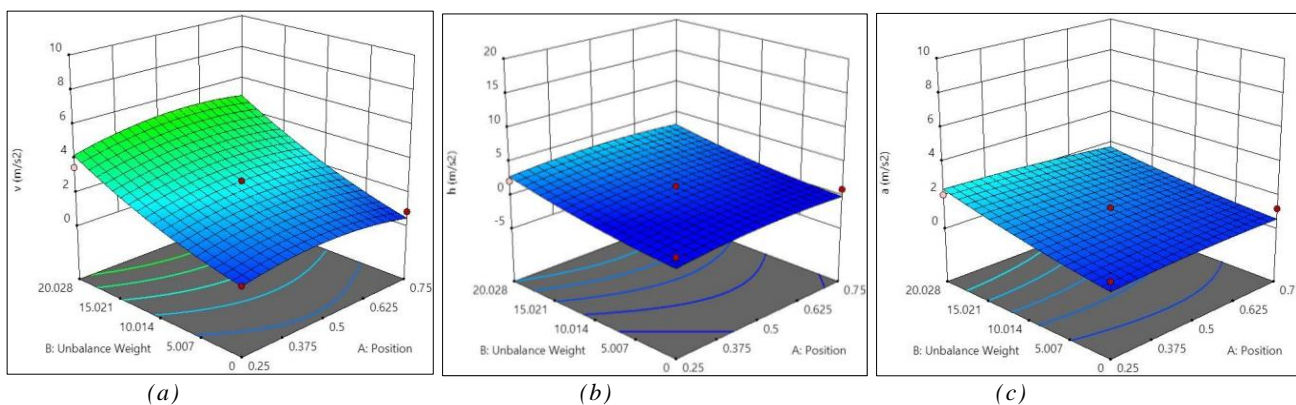


Figure 2. Response surface plot for (a) vertical response vs. unbalance weight, position (b) horizontal response vs. unbalance weight, position (c) axial response vs. unbalance weight, position.

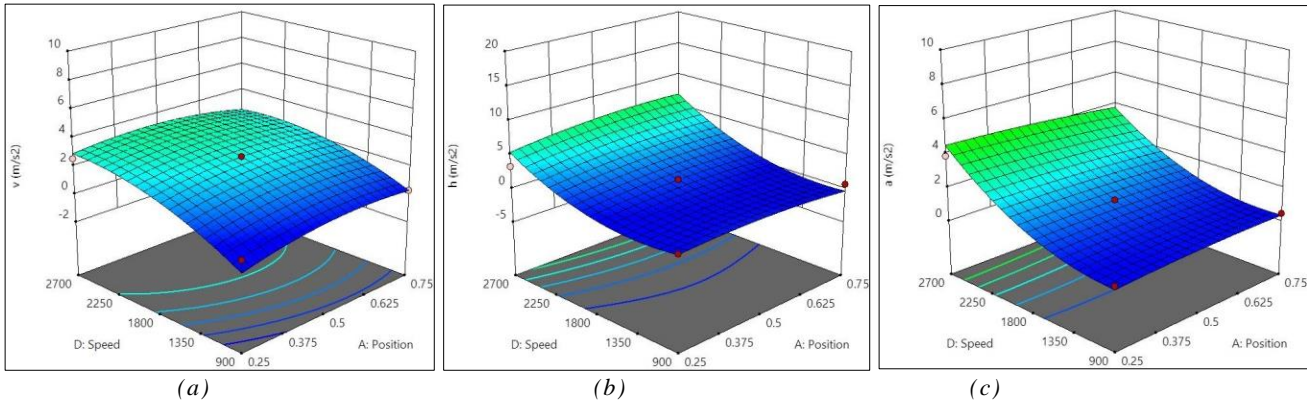


Figure 3. Response surface plot for (a) vertical response vs. speed, position (b) horizontal response vs. speed, position (c) axial response vs. speed, position.

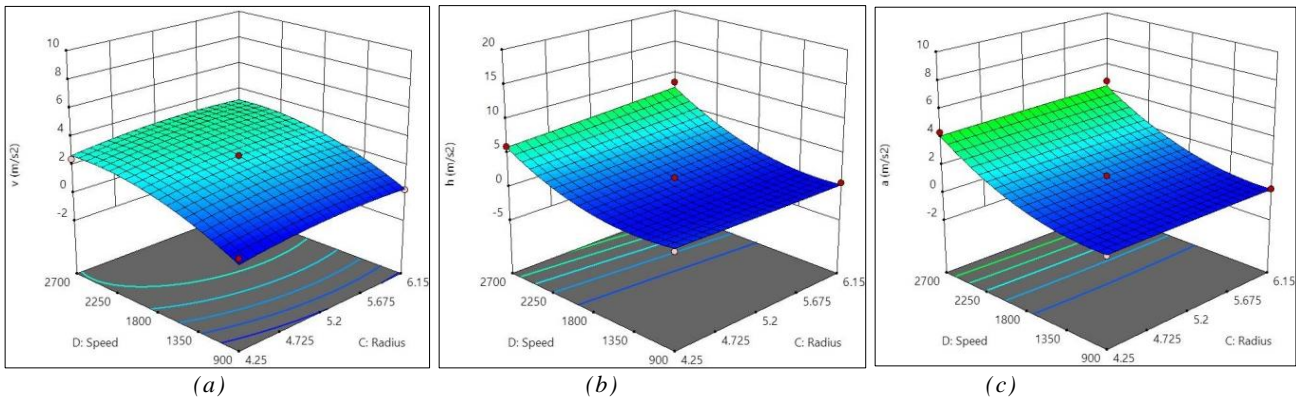


Figure 4. Response surface plot for (a) vertical response vs. speed, radius (b) horizontal response vs. speed, radius (c) axial response vs. speed, radius.

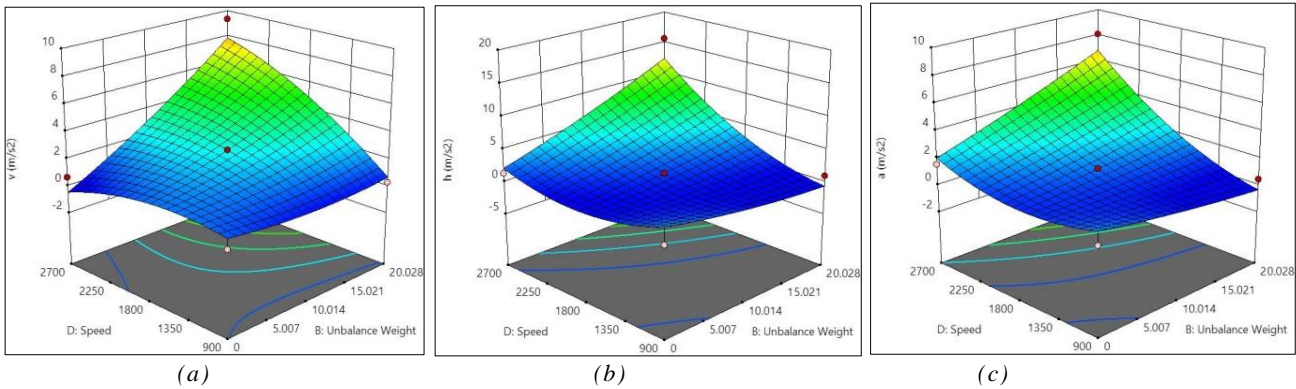


Figure 5. Response surface plot for (a) vertical response vs. speed, unbalance weight (b) horizontal response vs. speed, unbalance weight (c) axial response vs. speed, unbalance weight.

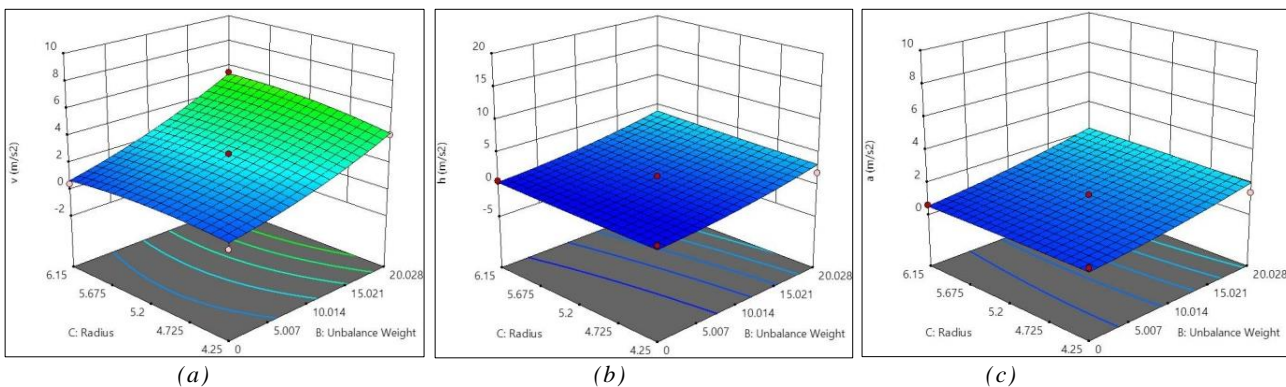


Figure 6. Response surface plot for (a) vertical response vs. radius, unbalance weight (b) horizontal response vs. radius, unbalance weight (c) axial response vs. radius, unbalance weight.

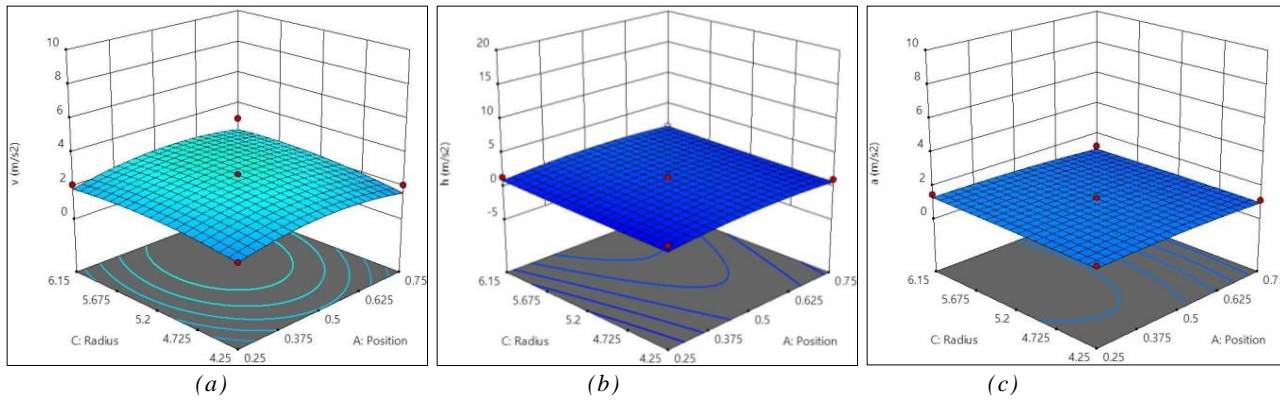


Figure 7. Response surface plot for (a) vertical response vs. radius, position (b) horizontal response vs. radius, position (c) axial response vs. radius, position.

For horizontal response, for position at 0.75, as the speed increases, the response increases from 0 m/s² at 900 rpm to 6.8 m/s² at 2700 rpm, similar trend is observed at position levels 1 and 2. Whereas with respect to position, for speed at 2700 rpm, response increases from 5 m/s² at position 0.25 m/s² to 7 m/s² at position 0.5 then decreases to 6.8 m/s² at position 0.75, similar trend is observed at speed levels 1 and 2. For axial response, for position at 0.75, as the speed increases, the response increases from 0.2 m/s² at 900 rpm to 3.8 m/s² at 2700 rpm of speed similar trend is observed at position levels 1 and 2. Whereas with respect to position, for speed at 2700 rpm, response decreases from 4.3 m/s² at position 0.25 m/s² to 4 m/s² at position 0.5 then decreases to 3.7 m/s² at position m/s², similar trend is observed at speed levels 1 and 2.

Figures 4(a), 4(b) and 4(c), represent the vertical, horizontal and axial responses vs. speed (factor D) and radius (factor C), where position (factor A) and unbalance weight (factor B) are held constant at 0.5 and 10.25 gm respectively. For vertical responses at 900 rpm speed, the response is constant with respect to radius, while at 2700 rpm speed, with respect to radius, the response increases from 2.5 m/s² at 4.25 cm to 3 m/s² at 6.15 cm. Now, with respect to speed, for radius at 6.15 cm, the response increases from 0 m/s² at 900 rpm to 3 m/s² at 2700 rpm. For horizontal responses at 900 rpm of speed, the response is constant with respect to radius, while at 2700 rpm of speed, with respect to radius, the response increases from 5.2 m/s² at 4.25 cm to 7.5 m/s² at 6.15 cm. Now, with respect to speed, for radius at 6.15 cm, the response increases from 0 m/s² at 900 rpm to 7.5 m/s² at 2700 rpm. For axial responses at 900 rpm of speed, the response is constant with respect to radius, while at 2700 rpm of speed, with respect to radius, the response increases from 4 m/s² at 4.25 cm to 4.4 m/s² at 6.15 cm. Now, with respect to speed, for radius at 6.15 cm, the response increases from 0 m/s² at 900 rpm to 4.15 m/s² at 2700 rpm.

Figures 5(a), (b) and (c) represent the vertical, horizontal and axial responses respectively vs. speed (factor D) and unbalance weight (factor B), where position (factor A) and radius (factor C) are held constant at 0.5 cm and 5.2 cm respectively. For vertical response, with respect to speed, for unbalance weight at 0 gm, the response remains constant at 0 m/s² while at 20.028 gm of unbalance weight, the response increases from 0.3 m/s² at 900 rpm to 7.8 m/s² at 2700 rpm of speed. Whereas with respect to unbalance weight, at 900 rpm of speed, response is constant at 0.2 m/s² while at 2700 rpm of speed the response increases from 0 m/s² at 0 gm to 7.8 m/s² at 20.028 gm of unbalance weight. For horizontal response, with respect to speed, at 0 gm of unbalance weight, the response varies from 2.5 m/s² at 900 rpm to 0 m/s² at 1800 rpm to 1.5 m/s² at 2700 rpm, while at 20.028 gm of unbalance weight, the response increases from 0.3 m/s² at 900 rpm to 7.8 m/s² at 2700 rpm of speed. Whereas with respect to unbalance weight, at 900 rpm of speed, response varies from 2.5 m/s²

at 0 gm to 0 m/s² at 20.028 gm, while at 2700 rpm of speed the response increases from 0 m/s² at 0 gm to 7.8 m/s² at 20.028 gm of unbalance weight. For axial response, with respect to speed, for unbalance weight at 0 gm, the response varies from 1 m/s² at 900 rpm to 0 m/s² at 1800 rpm to 2 m/s² at 2700 rpm, while at 20.028 gm of unbalance weight, the response increases from 0 m/s² at 900 rpm to 6.8 m/s² at 2700 rpm of speed. Whereas with respect to unbalance weight, at 900 rpm of speed, response varies from 1 m/s² at 0 gm to 0 m/s² at 20.028 gm, while at 2700 rpm of speed the response increases from 0 m/s² at 0 gm to 6.8 m/s² at 20.028 gm of unbalance weight.

Figures 6(a), 6(b) and 6(c) represent the vertical, horizontal and axial responses respectively vs. radius (factor C) and unbalance weight (factor B), where position (factor A) and speed (factor D) are held constant at 0.5 rpm and 1800 rpm respectively. For vertical response, with respect to radius, for unbalance weight at 0 gm, response remains constant at 0.3 m/s², while at 20.028 gm of unbalance weight, response increases from 4 m/s² at 4.25 cm to 5.4 m/s² at 6.15 cm of radius. Whereas with respect to unbalance weight, for radius at 6.15 cm, response increases from 0.5 m/s² at 0 gm to 5.4 m/s² at 20.028 gm, similar trend is observed at levels 1 and 2 of radius. For horizontal response, with respect to radius, for unbalance weight at 0 gm, response remains constant at 0 m/s², while at 20.028 gm of unbalance weight, response increases from 2.5 m/s² at 4.25 cm to 4 m/s² at 6.15 cm of radius. Whereas with respect to unbalance weight, for radius at 6.15 cm, response increases from 0 m/s² at 0 gm to 4 m/s² at 20.028 gm, similar trend is observed at levels 1 and 2 of radius. For axial response, with respect to radius, for unbalance weight at 0 gm, response remains constant at 0.5 m/s², while at 20.028 gm of unbalance weight, response increases from 2 m/s² at 4.25 cm to 2.4 m/s² at 6.15 cm of radius. Whereas with respect to unbalance weight, for radius at 6.15 cm, response increases from 0.5 m/s² at 0 gm to 2.4 m/s² at 20.028 gm, similar trend is observed at levels 1 and 2 of radius. Figures 7(a), (b) and (c) represent the vertical, horizontal and axial responses respectively vs. radius (factor C) and position (factor A), where unbalance weight (factor B) and speed (factor D) are held constant at 10.25 gm and 1800 rpm respectively. For vertical response, with respect to radius, for position at 0.75, response increases from 1.4 m/s² at 4.25 cm to 2.4 m/s² at 6.15cm, similar trend is observed at levels 1 and 2 of position. Whereas with respect to position, for radius at 6.15 cm, the response first increases from 1.8 m/s² at 0.25 to 2.6 m/s² at 0.5 then again decreases to 2 m/s² at 0.75, similar trend is observed at levels 1 and 2 of radius. For horizontal response, with respect to radius, for position at 0.75, response increases from 0.5 m/s² at 4.25 to 1.5 m/s² at 6.15, similar trend is observed at levels 1 and 2 of position. Whereas with respect to position, at 6.15 cm of radius, the response first increases from 1 m/s² at 0.25 m/s² to 1.5 m/s² at 0.5 then again decreases to 1 m/s² at 0.75, similar trend is observed

at levels 1 and 2 of radius. For axial response, with respect to radius, for position at 0.75, response remains constant at 1 m/s², similar trend is observed at levels 1 and 2 of position. Whereas with respect to position, at 6.15 cm of radius, the response varies from 1.1 m/s² at 0.25 m/s² to 1 m/s² at 0.75, similar trend is observed at levels 1 and 2 of radius.

5.2 Analysis of Variance

Analysis of Variance (ANOVA) tables are obtained from the Design Expert are observed to check the significant terms and their effect on the response. The DOE is done and the model is analysed for

quadratic model, hence the operating parameters are analysed up to 2 level interactions in ANOVA. The ANOVA tables for vertical, horizontal and axial responses are shown in Tables 4-6.

As it is observed from the Table 4, the p-values for the factors B unbalance weight is less than 0.0001, D speed is less than 0.0001, for interaction effect between factors B and D unbalance weight and speed is 0.0004, for D² is 0.0406, which are less than 0.05, hence the effect of these factors is significant. Hence, their contribution is to be considered.

Table 4. ANOVA table for vertical response.

Source	Sum of Squares	Degrees of freedom	Mean Square	F-value	p-value
Model	102.42	14	7.32	9.53	0.0002
A-Position	0.1856	1	0.1856	0.2419	0.6317
B-Unbalance Weight	48.46	1	48.46	63.14	<0.0001
C-Radius	0.7190	1	0.7190	0.9368	0.3522
D-Speed	24.95	1	24.95	32.52	<0.0001
AB	0.1793	1	0.1793	0.2336	0.6376
AC	0.0365	1	0.0365	0.0476	0.8309
AD	0.4578	1	0.4578	0.5965	0.4549
BC	0.4383	1	0.4383	0.5712	0.4644
BD	18.44	1	18.44	24.03	0.0004
CD	0.0002	1	0.0002	0.0003	0.9868
A ²	1.74	1	1.74	2.27	0.1576
B ²	0.9562	1	0.9562	1.25	0.2862
C ²	0.5792	1	0.5792	0.7548	0.4020
D ²	4.04	1	4.04	5.26	0.0406
Residual	9.21	12	0.7674		
Lack of Fit	9.21	10	0.9209		
Pure Error	0.0000	2	0.0000		
Cor Total	111.63	26			

Table 5. ANOVA table for horizontal response.

Source	Sum of squares	Degrees of freedom	Mean square	F-value	p-value
Model	240.28	14	17.16	5.28	0.0032
A-Position	0.4602	1	0.4602	0.1415	0.7134
B-Unbalance Weight	34.15	1	34.15	10.50	0.0071
C-Radius	1.02	1	1.02	0.3148	0.5851
D-Speed	114.37	1	114.37	35.17	<0.0001
AB	0.0282	1	0.0282	0.0087	0.9273
AC	0.0002	1	0.0002	0.0001	0.9935
AD	1.09	1	1.09	0.3358	0.5730
BC	0.0489	1	0.0489	0.0150	0.9044
BD	47.01	1	47.01	14.45	0.0025
CD	1.39	1	1.39	0.4279	0.5253
A ²	1.94	1	1.94	0.5967	0.4548
B ²	1.30	1	1.30	0.3997	0.5391
C ²	0.0122	1	0.0122	0.0038	0.9522
D ²	28.36	1	28.36	8.72	0.0121

Residual	39.03	12	3.25
Lack of Fit	39.03	10	3.90
Pure Error	0.0000	2	0.0000
Cor Total	279.30	26	

Table 6. ANOVA table for axial response.

Source	Sum of Squares	Degrees of freedom	Mean Square	F-value	p-value
Model	71.81	14	5.13	9.16	0.0002
A-Position	0.2382	1	0.2382	0.4256	0.5265
B-Unbalance Weight	7.03	1	7.03	12.55	0.0040
C-Radius	0.0067	1	0.0067	0.0119	0.9148
D-Speed	45.72	1	45.72	81.67	<0.0001
AB	0.1524	1	0.1524	0.2723	0.6113
AC	0.0050	1	0.0050	0.0089	0.9263
AD	0.2071	1	0.2071	0.3700	0.5543
BC	0.0365	1	0.0365	0.0652	0.8028
BD	10.48	1	10.48	18.72	0.0010
CD	0.0300	1	0.0300	0.0536	0.8208
A ²	0.0707	1	0.0707	0.1262	0.7285
B ²	0.1179	1	0.1179	0.2106	0.6545
C ²	0.0042	1	0.0042	0.0075	0.9322
D ²	6.11	1	6.11	10.91	0.0063
Residual	6.72	12	0.5598		
Lack of Fit	6.72	10	0.6717		
Pure Error	0.0000	2	0.0000		
Cor Total	78.53	26			

As it is observed from the Table 5, the p -values for the factors B unbalance weight is 0.0071, D speed is less than 0.0001, for interaction effect between factors B and D unbalance weight and speed is 0.0025, for D² is 0.0121, which are less than 0.05, hence the effect of these factors is significant. Hence, their contribution is to be considered.

As it is observed from the Table 6, the p -values for the factors B unbalance weight is 0.0040, D speed is less than 0.0001, for interaction effect between factors B and D unbalance weight and speed is 0.0010, for D² is 0.0063, which are less than 0.05, hence the effect of these factors is significant. Hence, their contribution is to be considered.

5.3 Regression Equations

Regression equation in coded units for vertical response is shown in Equation (6)

$$v = 2.70725 + 0.124369 * A + 2.00947 * B + 0.244772 * C + 1.44208 * D + 0.211705 * A * B + 0.095575 * A * C -$$

$$0.338286 * A * D + 0.331035 * B * C + 2.1471 * B * D - 0.007375 * C * D - 0.571708 * A^2 + 0.423418 * B^2 - 0.329552 * C^2 - 0.870208 * D^2 \quad (6)$$

Regression equation in coded units for horizontal response is shown in Equation (7)

$$h = +1.40 + 0.1958 * A + 1.69 * B + 0.2921 * C + 3.09 * D - 0.0840 * A * B - 0.0075 * A * C +$$

$$0.5225 * A * D + 0.1106 * B * C + 3.43 * B * D + 0.5899 * C * D - 0.6032 * A^2 + 0.4937 * B^2 + 0.0478 * C^2 + 2.31 * D^2 \quad (7)$$

Regression equation in coded units for axial response is shown in Equation (8)

$$a = +1.25 - 0.1409 * A + 0.7652 * B + 0.0236 * C + 1.95 * D - 0.1952 * A * B - 0.0353 * A * C - 0.2276 * A * D + 0.0955 * B * C + 1.62 * B * D + 0.0866 * C * D - 0.1151 * A^2 + 0.1487 * B^2 - 0.0281 * C^2 + 1.07 * D^2 \quad (8)$$

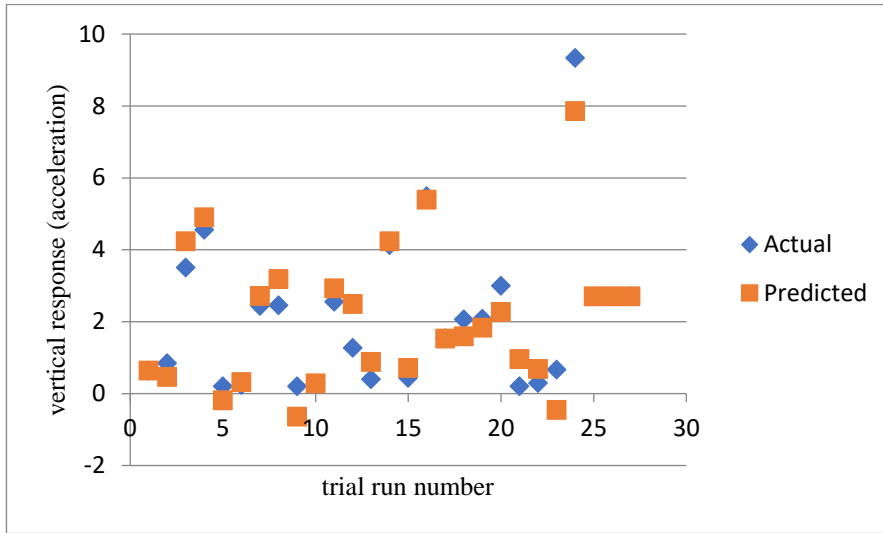


Figure 20. Actual vs. predicted values for vertical response.

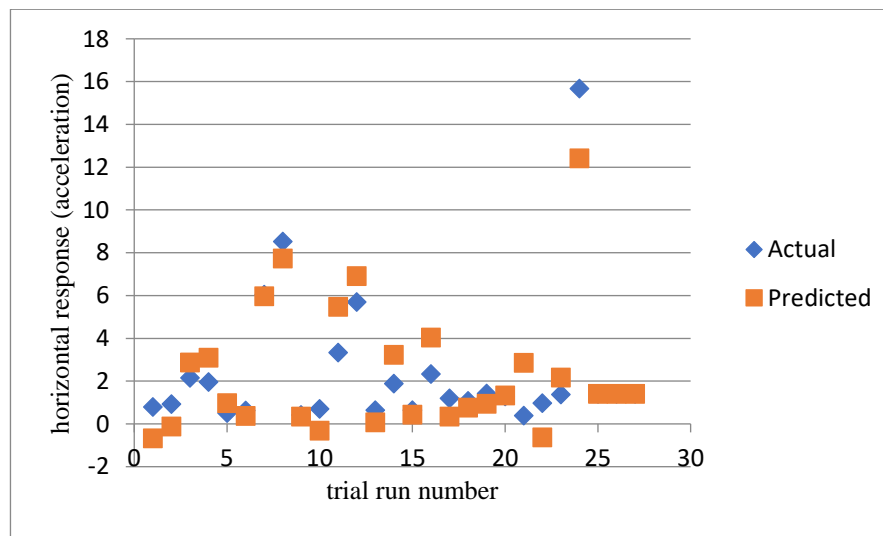


Figure 21. Actual vs. predicted values for horizontal response.

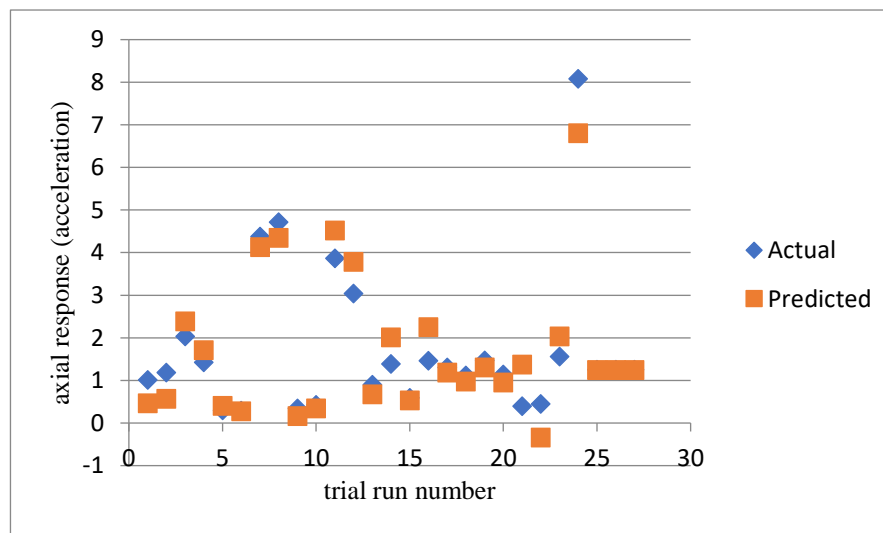


Figure 22. Actual vs. predicted values for axial response.

As seen from the Figures 20-22, we observe that the regression equation as predicted by Design Expert, quite predicts the response

satisfactorily. The deviation obtained from actual values can be due to the responses being of very low in magnitude of acceleration in m/s^2 .

6 Conclusion

The current work utilises Design of Experiments, Response Surface Method and ANOVA techniques to carry out several trials, investigating concurrent impact of operating factors on the unbalance in rotating machine with the aim to recognize the crucial operating factors, which affect the unbalance arising in the machine that is measured by the accelerometer sensors.

- The analysis of variance (ANOVA) unveiled that unbalance weight (factor B), speed (factor D) and interaction effect of B and D were significant.

- It is also quite evident from the Response Surface Plots, that the influence of radius (factor C) on the accelerometer sensor outputs was less significant.


- Hence, it is concluded that, the effect of unbalance on the rotating machine is dependent on the factors as, the responses (vertical, horizontal and axial) increase with the increase in unbalance weight, speed and radius, while at the centre position the responses are high as compared to the response when the disc is mounted at the quarter distance from the end position.

- The values predicted from the regression equations developed by the RSM model are found to be very close to the actual values measured from experimentation. The percentage error in predicted values is found to be 59.74% on average. This is due to the low value of magnitude of responses and testing conditions being dynamic and characteristics being non-linear.

Thus, the experimentation conducted and the results obtained have been successfully concluded as above. These conclusions are significant in deciding the contribution of the operating factors to the unbalance response arising in the rotating machine, which may further lead to bearing failure, incipient cracks, noise, reduced machine life, increased maintenance. Before-hand knowledge of the significant factors contributing to the unbalance can help in early detection and easy identification of factors so that the unbalance and thus vibrations arising out of it can be kept in check.

Acknowledgment: Authors would like to acknowledge L&T Infotech funding under CSR-1Step initiative and TEQIP-II (subcomponent 1.2.1) Centre of Excellence in Complex and Nonlinear Dynamical Systems (CoE-CNDS), VJTI, Matunga, Mumbai-400019, India for providing experimental environment.

References

1. Belhamra, A., Meramria, O., Kahine, K., Chehade, F. H., "Nonlinear Dynamical Analysis for a Plain Bearing," *Advances in Mechanical Engineering*, Vol. 6, 2014.
2. Erol, S. S., Meran, C., "Tribological approach on vibration and electrical current response of experimental misalignment and unbalance failure modes," *Journal of the Balkan Tribological Association*, Vol. 20, No. 4, pp. 559-575, 2014.
3. Jivkov, V. S., Zahariev, E. V., "Stability and non-stationary vibrations of rotor in elastoviscous field," *Mechanics Based Design of Structures and Machines*, Vol. 42, No. 1, pp. 35-55, 2014.
4. Di Lorenzo, R., Ingarao, G., Chinesta, F., "Integration of gradient based and response surface methods to develop a cascade optimisation strategy for Y-shaped tube hydroforming process design," *Advances in Engineering Software*, Vol. 41, pp. 336-348, 2010.
5. Kankar, P. K., Harsha, S. P., Kumar, P., Sharma, S. C., "Fault diagnosis of a rotor bearing system using response surface method," *European Journal of Mechanics-A/Solids*, Vol. 28, pp. 841-857, 2009.
6. Kankar, P. K., Sharma, S. C., Harsha, S. P., "Fault diagnosis of high speed rolling element bearings due to localized defects using response surface method," *Journal of Dynamic Systems, Measurement, and Control*, Vol. 133, No. 3, pp. 1-14, 2011.
7. Patil, P. P., Sharma, S. C., Jain, S. C., "Response surface modeling of vibrating omega tube (Copper) electromechanical coriolis mass flow sensor," *Expert Systems with Applications*, Vol. 39, pp. 4418-4426, 2012.
8. Kikuchi, S., Takayama, K., "Reliability assessment for the optimal formulations of pharmaceutical products predicted by a nonlinear response surface method," *International Journal of Pharmaceutics*, Vol. 374, pp. 5-11, 2009.
9. Zeng, G., Li, S. H., Yu, Z. Q., Lai, X. M., "Optimization design of roll profiles for cold roll forming," *Materials & Design*, Vol. 30, No. 6, pp. 1930-1938, 2009.
10. Liu, W., Yang, Y. Y., Xing, Z. W., Zhao, L. H., "Springback control of sheet metal forming based on the response surface method and multi-objective genetic algorithm," *Materials Science and Engineering A-Structural Materials Properties Microstructure and Processing*, Vol. 499, No. 1-2, pp. 325-328, 2009.
11. Sereshti, H., Karimi, M., Samadi, S., "Application of response surface method for optimization of dispersive liquid-liquid microextraction of water-soluble components of Rosa damascena Mill. Essential Oil," *Journal of Chromatogr A*, Vol. 1216, No. 2, pp. 198-204, 2009.
12. Rauf, M. A., Marzouki, N., Korbahti, B. K., "Photolytic decolorization of Rose Bengal by UV/H₂O₂ and data optimization using response surface method," *Journal of Hazard Mater*, Vol. 159, No. 2-3, pp. 602-609, 2008.
13. Tang, Y., Zhou, X., Chen, J., "Preform tool shape optimization and redesign based on neural network response surface methodology," *Finite Elements in Analysis and Design*, Vol. 44, No. 8, pp. 462-471, 2008.
14. Cheng, J., Li, Q. S., Xiao, R., "A new artificial neural network-based response surface method for structural reliability analysis," *Probabilistic Engineering Mechanics*, Vol. 23, No. 1, pp. 51-63, 2008.
15. Hou, T., Su, C., Liu, W., "Parameters optimization of a nano-particle wet milling process using the Taguchi method, response surface method and genetic algorithm," *Powder Technology*, Vol. 173, No. 3, pp. 153-162, 2007.
16. Tir, M., Moulai-Mostefa, N., "Optimization of oil removal from oily wastewater by electrocoagulation using response surface method," *Journal of Hazardous Materials*, Vol. 158, No. 1, pp. 107-115, 2008.
17. Choorit, W., Patthanamane, W., Manurakchinakorn, S., "Use of response surface method for the determination of demineralization efficiency in fermented shrimp shells," *Bioresource Technology*, Vol. 99, No. 14, pp. 6168-6173, 2008.
18. Montgomery, D. C., *Design and Analysis of Experiments*, 7th Edition, Hoboken, NJ, Wiley, 2009.
19. Box, G. E. P., Cox, D. R., "An analysis of transformation," *Journal of the Royal Statistical Society B*, Vol. 26, pp. 211-252, 1964.
20. Design Expert, Inc. Stat-Ease (Version 11), Veermata Jijabai Technological Institute, Mumbai, 2017-2018.
21. Matlab, Inc. Mathworks (Version R2017a), Veermata Jijabai Technological Institute, Mumbai, 2017-2018.
22. NVGate, OROS SASU, Veermata Jijabai Technological Institute, Mumbai, 2017-2018. 

The authors can be reached at: ammahadeshwar_m16@me.vjti.ac.in.